Annals of R.S.C.B., ISSN: 1583-6258, Vol. 25, Issue 4, 2021, Pages. 17361-17376
Received 20 May 2021; Accepted 03 June 2021

Electrochemical sensor for determination of Dopamine based on $MnCr_2O_4$ nanocomposites modified carbon paste electrode

S. R. Priyanka and K. P. Latha*
Department of P.G. Studies and Research in Chemistry, Sahyadri Science College (Autonomous), Constituent College of Kuvempu University, Shimoga-577203, Karnataka (S), INDIA
*Corresponding Author: K. P. Latha
E-mail address: kplatha11@gmail.com and priyankasr12345@gmail.com

Abstract

$MnCr_2O_4$ nanocomposites/modified carbon paste electrode based sensor were developed and validated by electrochemical detection of dopamine (DA). Hydrothermal method was used to prepare the $MnCr_2O_4$ nanocomposites. Various approaches were used to characterize the Synthesized $MnCr_2O_4$ nanocomposites. Cyclic voltammetry was used to investigate the redox properties of $MnCr_2O_4$ nanocomposites/modified carbon paste electrode ($MnCr_2O_4$ nanocomposites/MCPE). The oxidation and reduction peak occurred at pH7.4 with the supporting electrolyte being 0.2M phosphate buffer solution in the analysis of $MnCr_2O_4$ nanocomposites /MCPE. The $MnCr_2O_4$ nanocomposites/MCPE has a very low detection limit is 0.63 μM, high sensitivity, a large surface area, a wide linear range (10 μM to 100 μM), and good repeatability. This modified electrode, which was used to detect dopamine in injection samples, has a lot of promise in practical applications.

Keywords: Electrochemical sensors, $MnCr_2O_4$ nanocomposites, Dopamine, Injection Sample, Cyclic Voltammetry Study

1. Introduction

Dopamine (DA) is a modulator enzyme that plays an important role in neurotransmission. It is a catecholamine that belongs to the inhibitory neurotransmitter community. Also it is one of the most widely used catecholamines [1-2]. DA is generated by dopaminergic neurons in the ventral tegmental area, the midbrain, and the hypothalamic arcuate nucleus of the substantia nigra. DA is present near the periphery of the kidney, where it induces diuresis, natriuresis, and renal vasodilation. It helps with motor regulation and cognitive tasks including memory. DA is one of the most explored neurotransmitters due to its importance in the human body (e.g., human metabolism, cardiovascular, central nervous, renal, and hormonal systems) [3–9]. Since DA is essential for signal transmission to the brain, a deficit of it can cause a variety of neurological diseases and disorders, including schizophrenia, attention deficit hyperactivity disorder (ADHD), and Parkinson's disease (PD). The loss of DA-containing neurons will trigger this [10-16]. In both biochemical and clinical diagnostics, quantitative measurement of DA in human physiological fluids is essential. Chemiluminescence [17], fluorimetry [18], ultraviolet-visible spectrometry [19], and capillary electrophoresis (CE-luminescence) [20] are all methods for detecting DA. Because it is an electrochemically active molecule, DA may also be determined using electrochemical techniques [21]. Electrochemical methods have created a lot of attention in recent years because they can be used to detect the neurotransmitters rapidly, at a low cost, and with a low detection limit and high accuracy [22].

Many strategies for improving the determination of DA have recently been published, including electropolymerization [23], surfactant modified carbon paste electrode [24-25] chemically modified carbon paste electrodes [26] and metal oxide nanoparticles modified electrodes [27].

Annals of R.S.C.B., ISSN: 1583-6258, Vol. 25, Issue 4, 2021, Pages. 17361-17376
Received 20 May 2021; Accepted 03 June 2021

One of the most difficult tasks in modern surface science is to find effective modifiers for electrodes that can detect drug molecules. Researchers are interested in modifiers with low electrical conductivity, high surface area, long–term reliability, cost effectiveness, and high porosity [28–30]. Nanotechnology refers to the most dynamic control everywhere on the planet, and it is often regarded as the fastest-developing mechanical revolution in human history. Nanoscience is concerned with the study of materials and advancements in the range of 1-100 nanometers. Nanostructures and nanomaterials have been prepared using a variety of techniques. [31-32]. Metal oxides are exciting materials for basic research and electrochemical applications due to their wide range of synthetic properties. Oxides length a wide scope of electrical properties from extensive band-hole covers to metallic. Metal oxides are used in a wide range of applications, including sensors [33]. Modified electrodes as sensors have been widely employed in different electrochemical detection due to their remarkable qualities such as high centered field, good conductivity, sensitivity, reactivity, and stability. In recent years, researchers have been particularly interested in semiconductor nanoparticles because of their potential uses in material science [34].The present study describes, hydrothermal synthesis of $MnCr_2O_4$ nanocomposites, which was followed by characterization using X-ray diffraction (XRD), Energy Dispersive X-Ray (EDX) Analysis, Fourier transformer infrared spectroscopy (FTIR), Ultra violet visible (UV-Visible) spectroscopy, and Scanning electron microscope (SEM) analysis. Then, $MnCr_2O_4$ nanocomposites/MCPE was prepared by mixing 6mg of $MnCr_2O_4$ nanocomposites with 70%:30% ratio of carbon paste electrode. This $MnCr_2O_4$ nanocomposites/MCPE were used for electrochemical detection of Dopamine (DA), at 0.2M PBS as used for supporting electrolyte (pH=7.4). The $MnCr_2O_4$ nanocomposites/MCPE has good electrocatalytic activity, a large electroactive surface area, high sensitivity, a low detection limit and minimization in over potential for DA.

2. Experimental section

2.1. Apparatus and chemical reagents

All tests have been carried out on a CHI-660c electrochemical work station potentiostat. A three-electrode cell with a bare carbon paste electrode (BCPE) and $MnCr_2O_4$ nanocomposites modified carbon paste electrode ($MnCr_2O_4$ nanocomposites/MCPE) as working electrodes, a saturated calomel electrode (SCE) as a reference electrode, and a platinum wire as an auxiliary electrode was used for the electrochemical measurements. All of the oxidation potential values obtained are plotted against SCE. Himedia provided dopamine (DA) (Bangalore, India). In double deionised water, a stock solution of DA (25×10^{-4}M) is prepared. Loba chemie and Himedia provided graphite powder (50m particle size) and silicone oil, respectively (Bangalore,India). All of the chemicals were of analytical grade. Merck (Bangalore, India) supplied the ingredients for the preparation of buffer solutions and $MnCr_2O_4$ nanocomposites preparation. Standard stock solutions of 0.2M $NaH_2PO_4.H_2O$ and 0.2M Na_2HPO_4 were mixed with double deionised water to make the 0.2M phosphate buffer solution (PBS) and Manganese chloride ($MnCl_2$), potassium chromate (K_2CrO_4), sodium nitrate ($NaNO_3$). Prior to analysis, both of the solutions were freshly prepared. The DA injection sample purchased from sterile specialities India Private Ltd with a specified content of DA of 40.0 mg/mL.

2.2. Preparation of Manganese (II) Chromate ($MnCr_2O_4$) nanocomposites

Hydrothermal method was used for the synthesis of $MnCr_2O_4$ nanocomposites. For that 1:1 ratio, of manganese chloride ($MnCl_2$) and potassium chromate (K_2CrO_4) were taken in the round

Annals of R.S.C.B., ISSN: 1583-6258, Vol. 25, Issue 4, 2021, Pages. 17361-17376
Received 20 May 2021; Accepted 03 June 2021

bottom flask and it was liquefied in a 50 mL deionized water. Fallowing that, 0.7 g of sodium hydroxide (NaOH) was combined and sonicated for three h accordingly, after which the mixture was placed in a Teflon-autoclave for 20 h and kept at 210 ^{0}C. Finally, centrifugation was used to separate the products, which were then dried at 60 ^{0}C. Furthermore, the particles were separated from solution by centrifugation, and rinsed with double distilled water and ethanol, and then dried for 24 h at 100 ^{0}C. Then obtained product was $MnCr_2O_4$ nanocomposites.

2.3. Preparation of bare carbon paste electrode

The bare carbon paste electrode (BCPE) was made with a 70:30 (w/w) mixture of graphite powder and silicone oil, ground for 30 minutes in an agate mortar and pestle to obtain a compatible carbon paste. After that, a small amount of the prepared paste was stuffed tightly into the cavity of a Teflon tube and smoothed with zero grade butter paper. A copper wire was used to make an electrical connection.

2.4. Preparation of $MnCr_2O_4$ nanocomposites modified carbon paste electrode ($MnCr_2O_4$ nanocomposites/MCPE)

To make the modified carbon paste electrode, an agate mortar was used to blend the 6mg of $MnCr_2O_4$ nanocomposites, 70:30 (w/w) graphite powder, and silicone oil to make a homogeneous paste. A copper wire was inserted to maintain electrical contact after a portion of the paste was stuffed tightly into the cavity of a Teflon tube. The paste's surface was polished with a zero-grade butter paper until it was gleaming.

3. Results and Discussion

3.1. Characterization of $MnCr_2O_4$ nanocomposites

The XRD pattern of $MnCr_2O_4$ nanocomposites are shown in Figure.1 (Fig.1). In XRD pattern of $MnCr_2O_4$ nanocomposites the peaks appear at 2 theta=18.8^0, 29.21^0, 34.39^0, 41.78^0, 51.79^0, 55.19^0, 60.57^0, 64.67^0, 68.64^0, 72.51^0 and 76.29^0 corresponds to (111), (220), (311), (400), (422), (511), (440), (442), (620), (622) and (444) planed respectively and also corresponds to the crystalline structure of $MnCr_2O_4$ nanocomposites [35]. The strongest reflection occurs at the plane (311) is the characteristic phase of $MnCr_2O_4$ nanocomposites which confirms the formation of $MnCr_2O_4$ nanocomposites. The observed XRD data confirm the successful synthesis of $MnCr_2O_4$ nanocomposites.

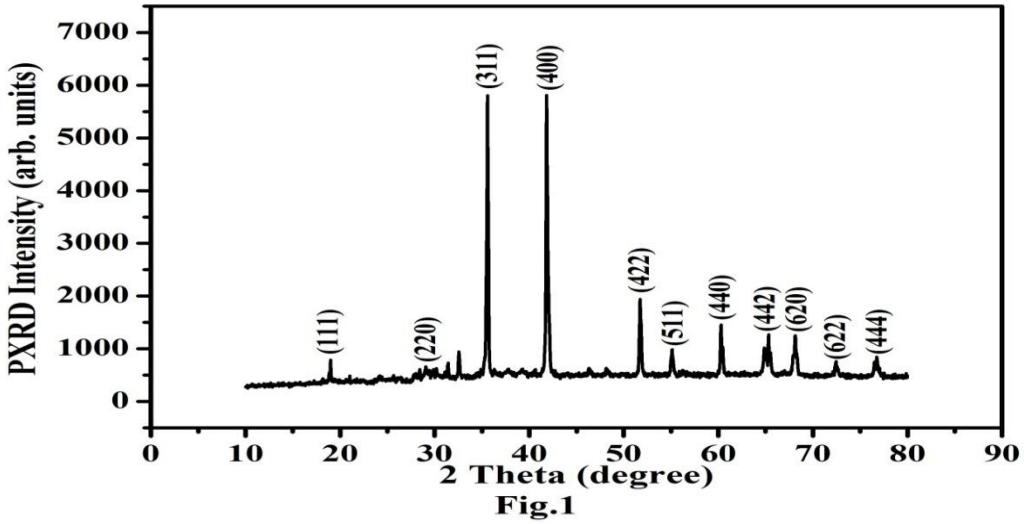

Fig.1. XRD pattern of $MnCr_2O_4$ nanocomposites

Annals of R.S.C.B., ISSN: 1583-6258, Vol. 25, Issue 4, 2021, Pages. 17361-17376
Received 20 May 2021; Accepted 03 June 2021

The EDX analysis validated the stoichiometric elemental content and purity of the produced samples. The EDX spectra in Fig. 2 indicate intensity peaks associated with Mn in addition to Cr and O. This proves that the synthesis was impurity-free and that the $MnCr_2O_4$ phase was pure. Table 1 shows that the at% and wt % of all elements are exactly the same as their stoichiometric composition in their respective formula units [36].

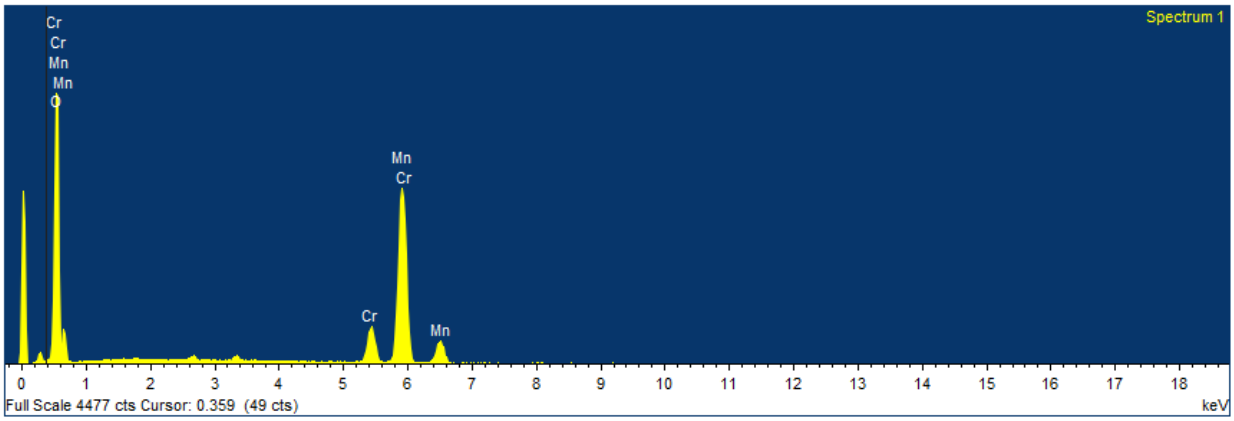

Fig.2

Fig.2. EDX spectra of $MnCr_2O_4$ nanocomposites sample

Table 1. Quantitative data of wt% and at% of the entire element in $MnCr_2O_4$ nanocomposites.

Element	wt%	at%
Mn	54.81	29.07
Cr	09.00	05.04
O	36.19	65.84

The IR spectra of $MnCr_2O_4$ nanocomposites are shown in Fig.3. The metal's Mn-O vibration frequency at tetrahedral clearance and octahedral clearance are ascribed to two absorption peaks at 518 cm^{-1} and 620 cm^{-1}, respectively[37].

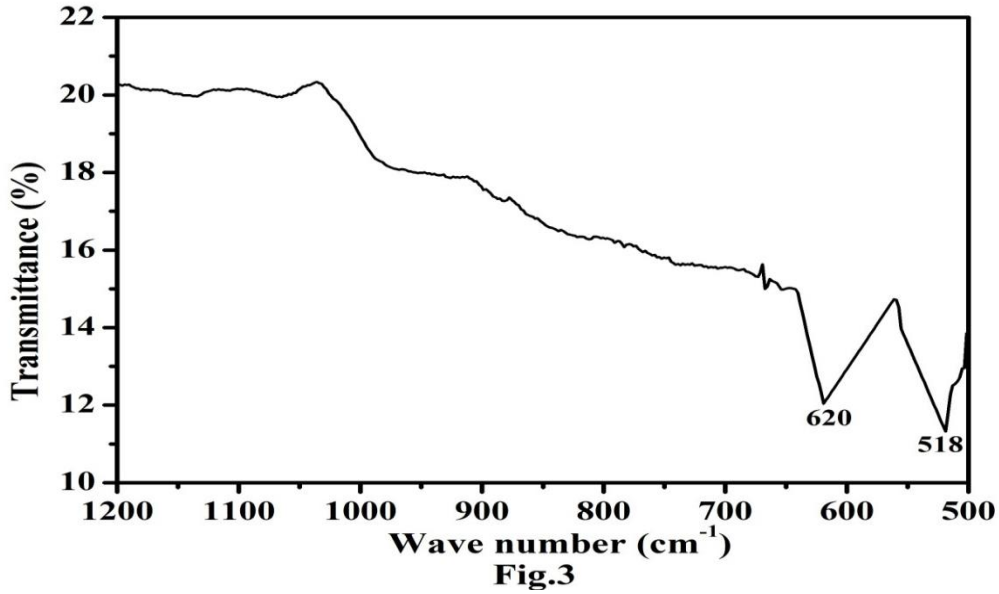

Fig.3. IR spectrum of the $MnCr_2O_4$ nanocomposites

Annals of R.S.C.B., ISSN: 1583-6258, Vol. 25, Issue 4, 2021, Pages. 17361-17376
Received 20 May 2021; Accepted 03 June 2021

The surface morphology and particle size of the as prepared $MnCr_2O_4$ nanocomposites were further analyzed by FE-SEM. From the FE-SEM images as shown in Fig.4, it was observed that the $MnCr_2O_4$ nanocomposites were well decorated as homogeneous particles and the estimated cluster size was ~ 100 nm. The SEM image of the $MnCr_2O_4$ nanocomposites shows nanoclusters were sandwich sheets, which is good evidence for the stable electrode operations during the conversion reaction. The monotone $MnCr_2O_4$ nanocomposites are located as surface layers. The suitable interaction between $MnCr_2O_4$ nanocomposites and flake-like sheets limits the aggregation of crystalline $MnCr_2O_4$ nanocomposites [36]

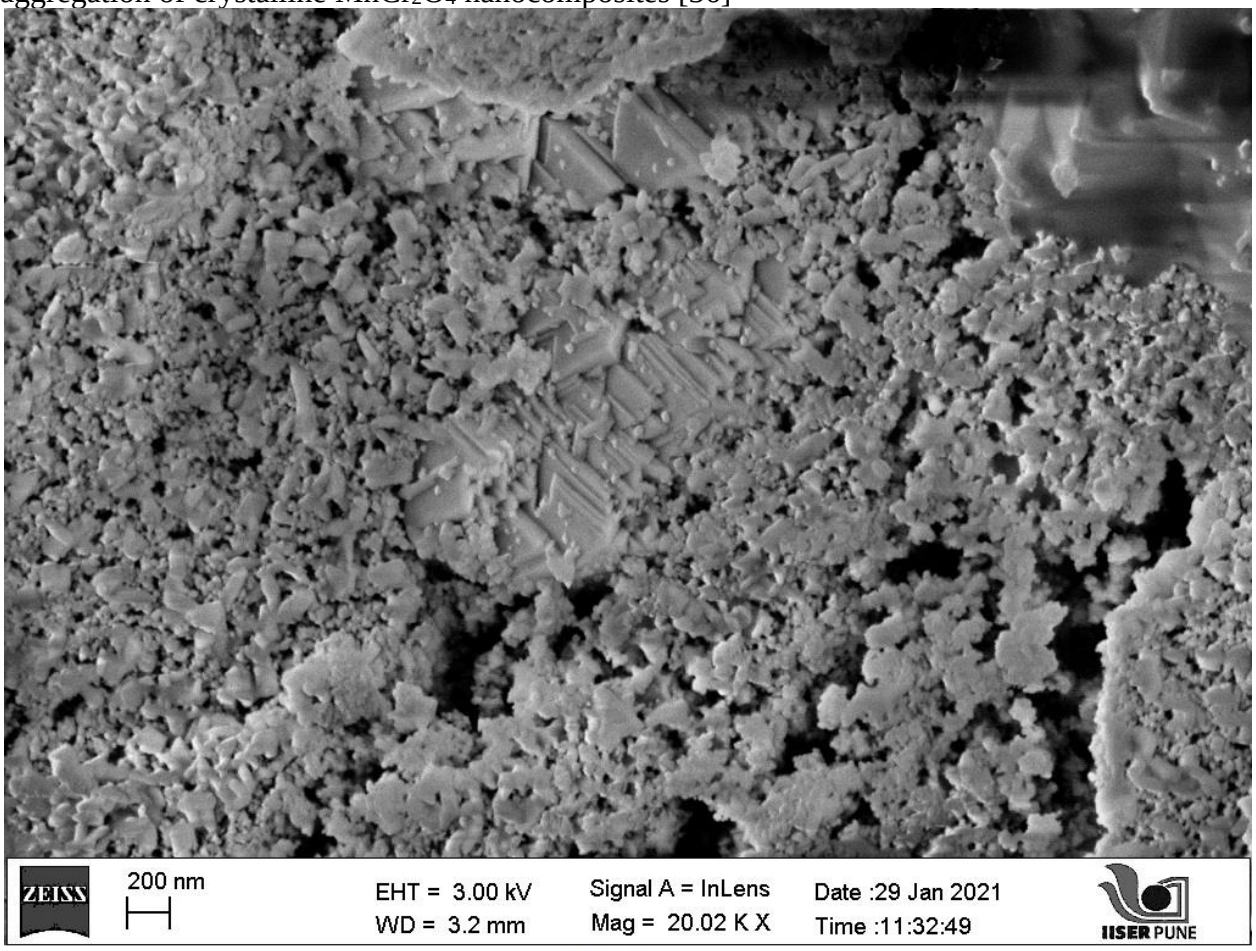

Fig.4

Fig.4. SEM image of $MnCr_2O_4$ nanocomposites.

3.2. Electrochemical behavior of Potassium ferrocyanide at BCPE and $MnCr_2O_4$ nanocomposites/MCPE

The cyclic voltammetry (CV) response of the $MnCr_2O_4$ nanocomposites//MCPE and BCPE was studied at freshly prepared 1 mM Potassium ferrocyanide ($K_4[Fe(CN)_6]$) in 1 M potassium chloride (KCl) solution at the sweep rate $50mVs^{-1}$ as shown in Fig.5, directs the CV response of $MnCr_2O_4$ nanocomposites//MCPE (dashed line) at 1mM ($K_4[Fe(CN)_6]$) shows good response with high redox current signal, the redox peak potential appeared at Epa=263mV and Epc=194mV respectively. The change in the peak potential (ΔEp= Epa- Epc) of modified electrode is 69mV. However, the BCPE (solid line) provides very low redox current signal, with Epa=267mV and Epc=190mV as the redox peak potentials, respectively. The change in peak potential difference of

Annals of R.S.C.B., ISSN: 1583-6258, Vol. 25, Issue 4, 2021, Pages. 17361-17376
Received 20 May 2021; Accepted 03 June 2021

BCPE is ΔEp=77mV. The minimization of redox peak potential with enhancement in redox peak shows the electrocatalytic behavior of $MnCr_2O_4$ nanocomposites/MCPE towards $K_4[Fe(CN)_6]$. The fabricated $MnCr_2O_4$ nanocomposites/MCPE and BCPE were studied at various scan rates [50 to 500 mVs^{-1}] under identical condition of 1mM potassium ferrocyanide ($K_4[Fe(CN)_6]$) in 1 M KCl solution as a supporting electrolyte,. The active surface area of electrodes for reversible processes can be determined using Randles-equation Sevick's (1) [38-40].

$$I_p = (2.69 \times 10^5)\, n^{3/2}\, A\, D^{1/2}\, C_0 \upsilon^{1/2} \text{ ----- (1)}$$

Where, I_p is the peak current, A is the electroactive surface area (cm^2), C_0 is the concentration of the electroactive species ($molcm^{-3}$), n is the number of exchanged electrons, D is the diffusion coefficient (cm^2s^{-1}) and υ is the scan rate (Vs^{-1}). The diffusion controlled mechanism is shown by the observed linear relationship of the oxidation peak currents as a function of the square root of the scan. The values of A for $MnCr_2O_4$ nanocomposites/MCPE and BCPE, respectively, are 0.0460 cm^2 and 0.029 cm^2 based on the slope I_{pa} versus $\upsilon^{1/2}$.

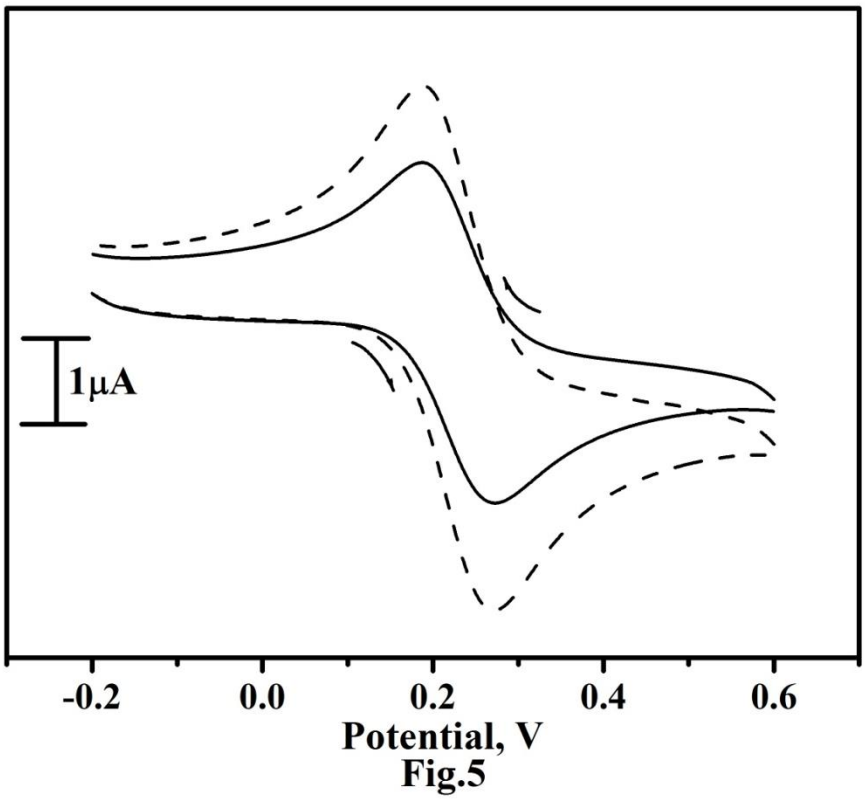

Fig.5

Fig.5. Cyclic voltammograms for 1mM $K_4[Fe(CN)_6]$ and supporting electrolyte 1M KCl at BCPE (solid line) and $MnCr_2O_4$ nanocomposites/MCPE (dashed line) with scan rate of $50mVs^{-1}$. **3.3. The sensor DA**

The electrochemical responses of 10μM DA in 0.2 M phosphate buffer solution (0.2M PBS) of pH 7.4 at the BCPE (dashed line) and at the $MnCr_2O_4$ nanocomposites/MCPE (solid line) were measured at a scan rate of $50mVs^{-1}$. The possible mechanism for DA undergoes oxidation to give dopamine ortho semiquinone (Dopamine o-semiquinone) as shown in scheme.1.The difference in peak potential for $MnCr_2O_4$ nanocomposites/MCPE was 53mV and for BCPE was 72mV. The corresponding anodic peak currents were 5.17×10^{-7} A and 1.11×10^{-6}A for the bare CPE and $MnCr_2O_4$ nanocomposites/MCPE respectively, has been shown in Fig. 6. The result showed $MnCr_2O_4$ nanocomposites/MCPE minimizes the over potential with enhancing

Annals of R.S.C.B., ISSN: 1583-6258, Vol. 25, Issue 4, 2021, Pages. 17361-17376
Received 20 May 2021; Accepted 03 June 2021

the redox peak current. This indicated that the $MnCr_2O_4$ nanocomposites/MCPE exhibited good electrocatalytic activity towards the detection of DA.

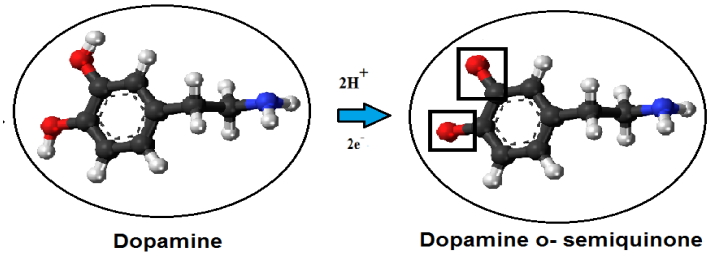

Scheme.1. Tentative electrochemical oxidation of DA.

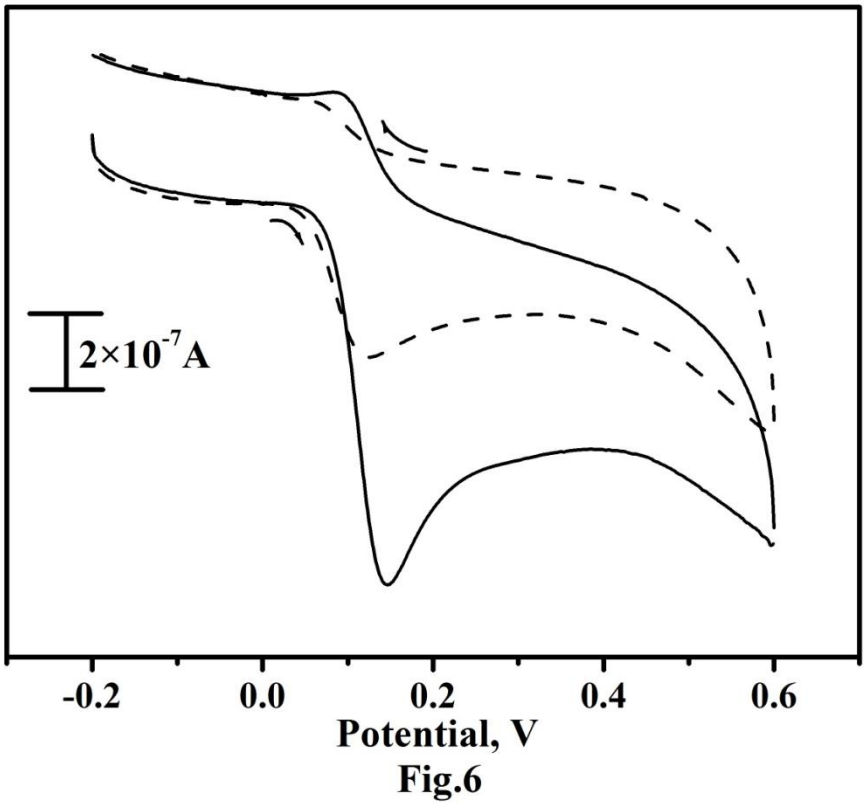

Fig.6. CVs of 10µM DA in 0.2M PBS of pH 7.4 at BCPE (dashed line) and $MnCr_2O_4$ nanocomposites/MCPE (solid line) with the scan rate of $50mVs^{-1}$.

3.4 Effect of scan rate

Fig. 7A shows the result of changing the scan rate for 10µM DA in 0.2 M PBS on $MnCr_2O_4$ nanocomposites/MCPE in the potential range of 0.2 to 0.6V. Over the studied range of 50 to 500 mVs^{-1}, the anodic peaks increased with a marginal positive shift in the peak potential and showed linearity with the scan rate. The slope value for DA was 0.638 for logarithmic anodic peak current (logIpa) versus logarithmic of scan rate (logυ) (Fig 7B), which is close to the theoretical value of 0.5 for diffusion controlled method for $MnCr_2O_4$ nanocomposites/MCPE [41]. The plot of anodic peak current (Ipa) of DA versus square root of scan rate ($\upsilon^{1/2}$) is shown in Fig. 7C. With a

Annals of R.S.C.B., ISSN: 1583-6258, Vol. 25, Issue 4, 2021, Pages. 17361-17376
Received 20 May 2021; Accepted 03 June 2021

correlation coefficient (r^2) of 0.9903, the resulting graph showed excellent linearity. Using the difference in the peak potential (ΔE_p) from the experimental data and equation (2) [42, 43], the heterogeneous rate constant (k^0) values for DA were determined and it shows the increasing the scan rate k^0 also increases which confirms the electrode process was controlled by diffusion. The Difference in redox peak potential (ΔE_p) values and the respective values of the k^0 for the oxidation DA are listed in Table 2 for $MnCr_2O_4$ nanocomposites/MCPE.

$$\Delta E_p = 201.39 \log (\upsilon / k^0) - 301.78 \quad \text{---------} \quad (2)$$

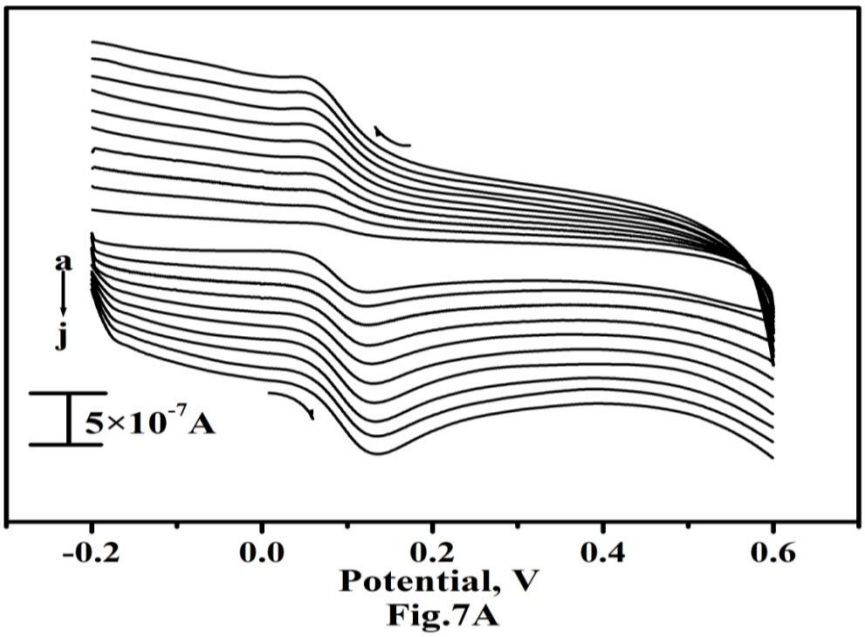

Fig.7A. CVs of 10µM DA in 0.2M PBS of pH 7.4 with different scan rates at $MnCr_2O_4$ nanocomposites/MCPE (a-j; 50mVs^{-1}to 500 mVs^{-1}).

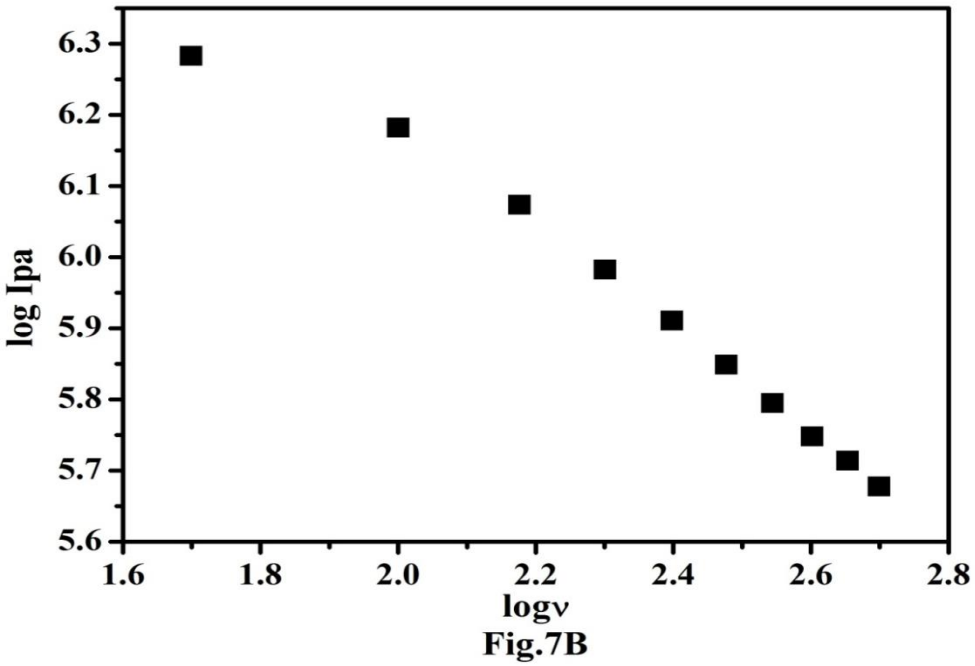

Fig.7B. Graph of log I_{pa} of DA versus log υ.

Annals of R.S.C.B., ISSN: 1583-6258, Vol. 25, Issue 4, 2021, Pages. 17361-17376
Received 20 May 2021; Accepted 03 June 2021

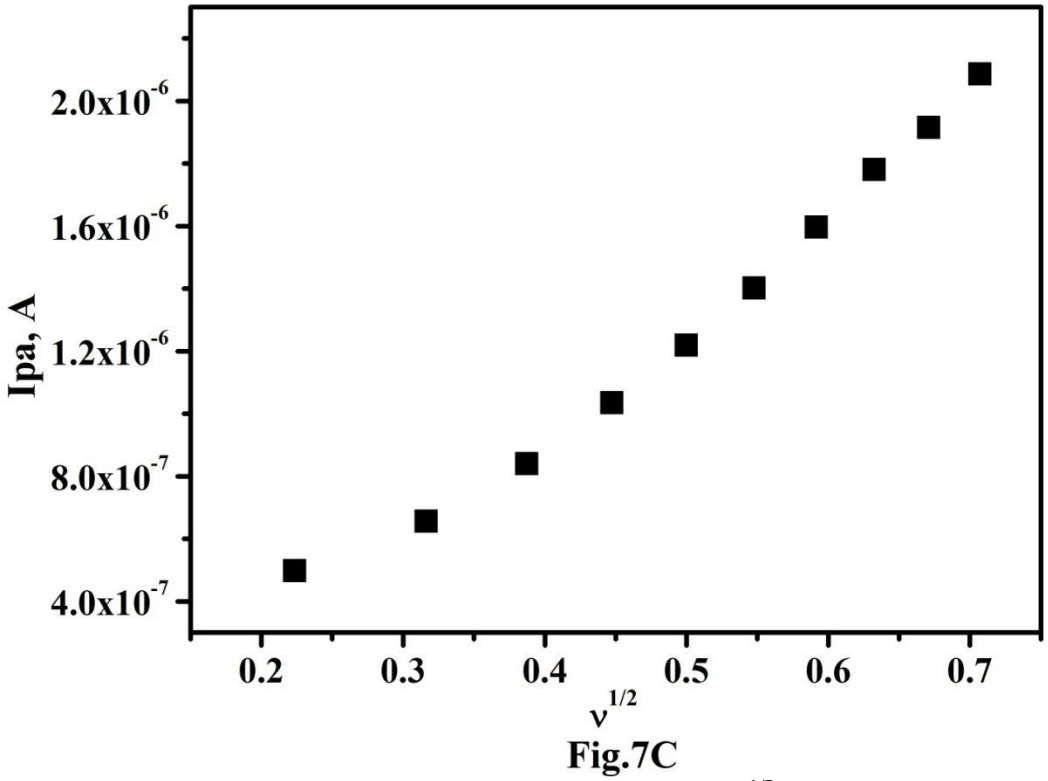

Fig.7C. Graph of I_{pa} of DA versus $\upsilon^{1/2}$.

Table.2. Determination of the heterogeneous rate constant (k^0) values for DA

υ/mVs^{-1}	ΔE_p/mV	k^o / s^{-1}
50	57.6	0.8195
100	59.3	1.6110
150	60.7	2.3784
200	61.1	3.1564
250	63.7	3.8291
300	66.2	4.4660
350	69.9	4.9945
400	73.2	5.4960
450	74.8	6.0715
500	77.8	6.5177

3.5. Concentration Effect of DA at $MnCr_2O_4$ nanocomposites/MCPE

The Fig.8A shows the CVs of DA by varying its concentration from a linear dynamic range of 10µM to 90µM in 0.2M PBS of pH 7.4 with a scan rate of 50mVs^{-1}at $MnCr_2O_4$ nanocomposites/MCPE in the potential range of -0.2 to 0.6V. The Ipa and Ipc increased linearly as the concentration of DA increased. The Ipa and Ipc continue to rise, with E_{pa} shifting to a more positive side and E_{pc} to a less negative side. E_{pa} shifted from 283 to 177 mV, while E_{pc} shifted from 59 to 74 mV. The linearity and correlation co-efficient value of (r^2) = 0.9932 is used to plot the graph of Ipa versus DA concentration in Fig.8B. The limits of detection (LOD) and quantification (LOQ) were 0.63µM and 2.1µM, respectively. The LOD was calculated according to the equation

Annals of R.S.C.B., ISSN: 1583-6258, Vol. 25, Issue 4, 2021, Pages. 17361-17376
Received 20 May 2021; Accepted 03 June 2021

$LOD = KS^0/S$, where K is a constant related to the confidence level. In accordance with the suggestion of the IUPAC, the value of K is 3 at the 99% confidence level, S^0 is the standard deviation of six blank-solution measurements (no added DA), and S is the slope of the calibration graph. The proposed electrode exhibited a relatively lower detection limit than those recently reported elsewhere [43-47] (Table 3).

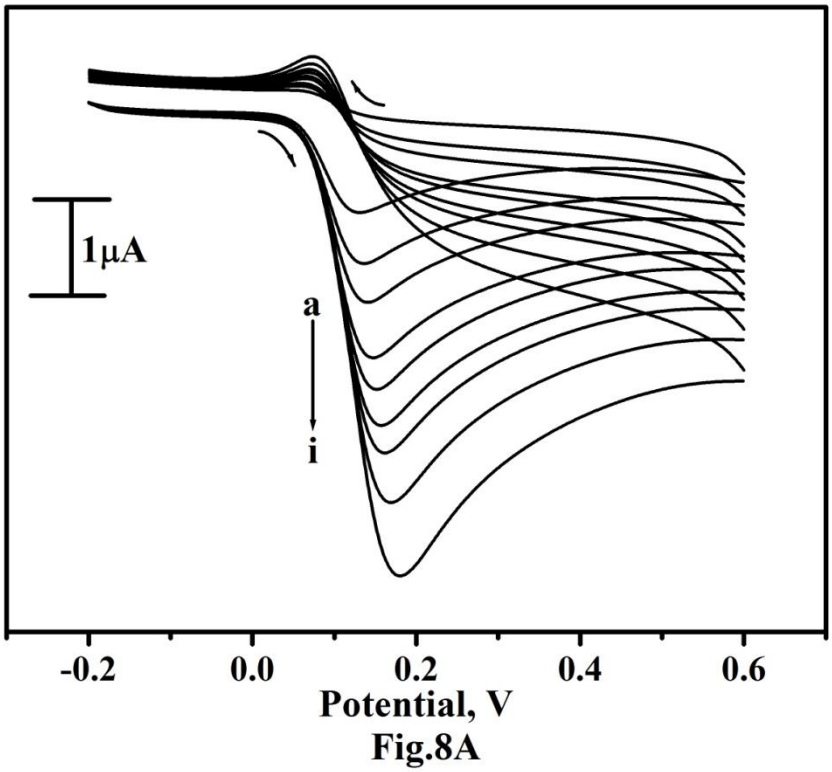

Fig.8A

Fig.8A. CVs for different concentrations of DA (a-j; 10μM to 90μM) in 0.2M PBS of pH 7.4 with scan rate 50mVs^{-1}at $MnCr_2O_4$ nanocomposites/MCPE.

Electrode	Detection limit(μM)	Techniques	Reference
SDS/polyglycine/phthalamide/CPE	1.51	DPV	[43]
Banana/MWCNTs/MCPE	2.09	DPV	[44]
LDH/CILE	5.0	DPV	[45]
CTAB/CPE	11.0	DPV	[46]
Metallothioneins self assembled gold electrode	6.0	CV	[47]
$MnCr_2O_4$ nanocomposites/MCPE	0.63	CV	This Paper

Annals of R.S.C.B., ISSN: 1583-6258, Vol. 25, Issue 4, 2021, Pages. 17361-17376
Received 20 May 2021; Accepted 03 June 2021

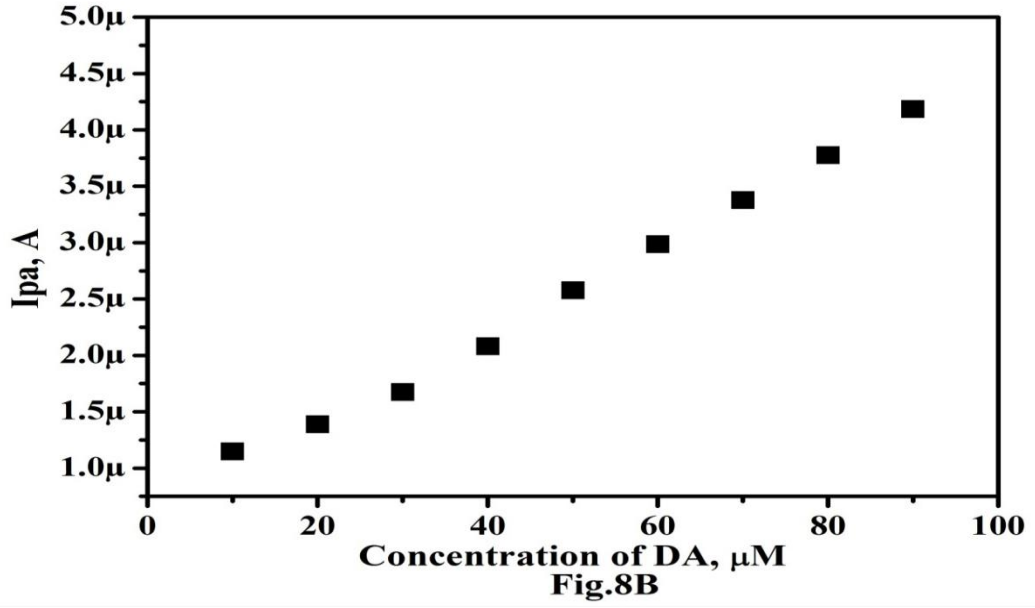

Fig.8B. Graph of I_{pa} versus concentration of DA

Table 3. Comparison of the detection of different modified electrodes

3.6 pH dependence study of DA at $MnCr_2O_4$ nanocomposites/MCPE

The focus of the CV study was performed to investigate the effect of supporting electrolyte towards the electrochemical oxidation of 10µM DA at $MnCr_2O_4$ nanocomposites/MCPE. Electrochemical analysis was performed in 0.2 M PBS at varied pH (5.8 - 7.4) with the scan rate of 50 mVs^{-1} as shown in Fig.9A. Increasing the pH value from 5.8 to 7.4 causes the Epa of DA to shift to the negative side. The potential diagram was generated by plotting a graph of Epa versus pH values as shown in Fig.9B. The graph has good linearity with a slope of 67mV/pH, this behavior is nearly obeyed the Nernst Equation for transfer of two protons and electrons were engaged in the electrochemical reaction of DA [41, 43].

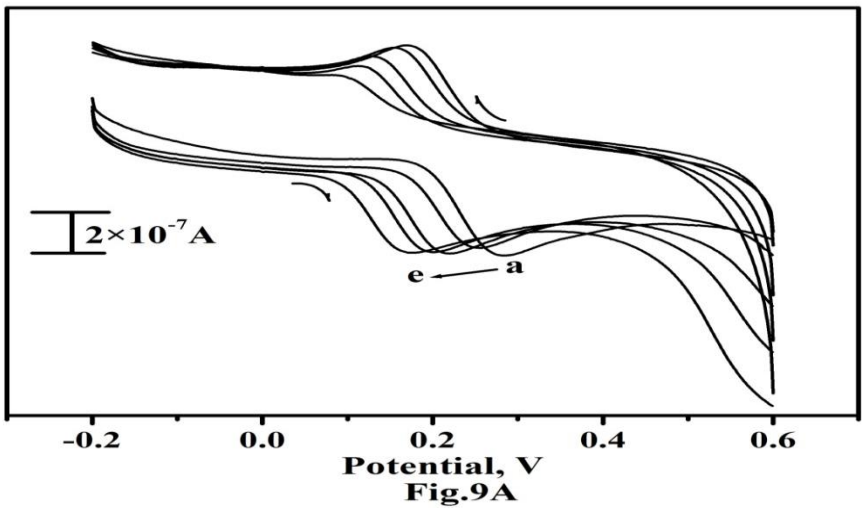

Fig.9A. Cyclic voltammograms of 10µM DA for variation of pH from 5.8 to 7.4 at 0.2M PBS Solution at $MnCr_2O_4$ nanocomposites/MCPE, Scan rate: 50mVs^{-1}.

Annals of R.S.C.B., ISSN: 1583-6258, Vol. 25, Issue 4, 2021, Pages. 17361-17376
Received 20 May 2021; Accepted 03 June 2021

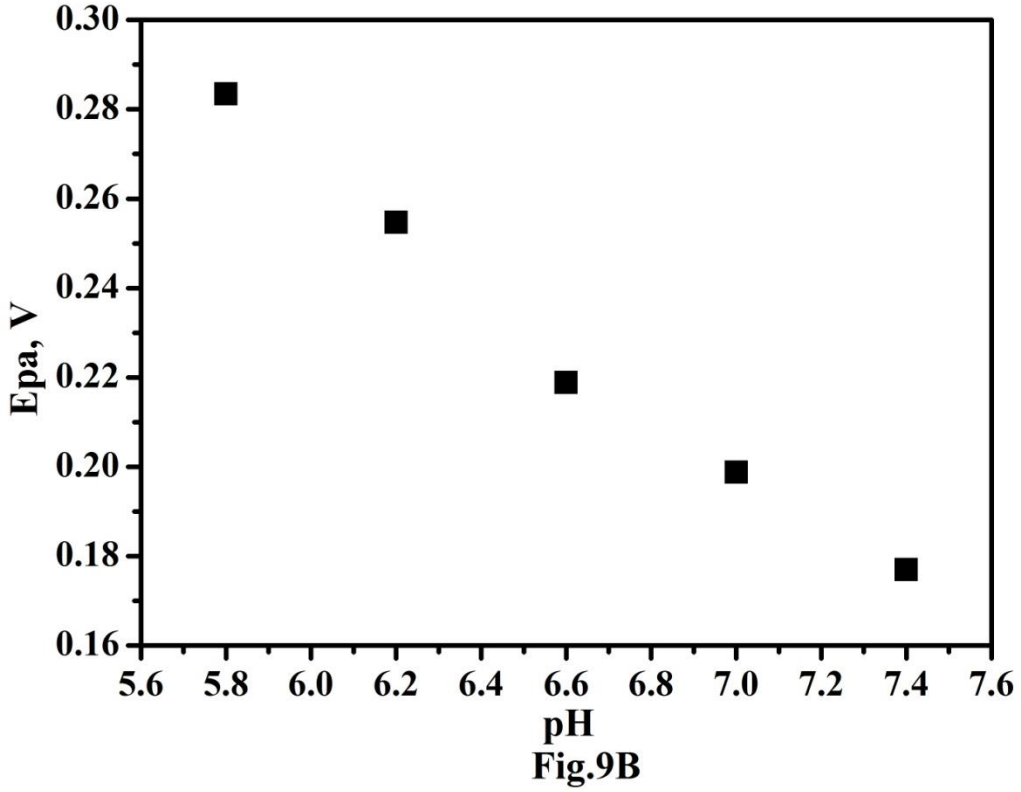

Fig.9B. Graph of Epa v/s pH

3.7. Analytical applications

The $MnCr_2O_4$ nanocomposites/MCPE was applied in the analysis of DA containing injection samples. The DA injection sample purchased from sterile specialities India Private Ltd with a specified content of DA of 40.0 mg/mL. After a proper dilution, the sample was utilized. The injection samples were dilute with 0.2 M PBS. Table 4 summarizes the findings. The recovery and R.S.D. were satisfactory, indicating that the suggested approaches may be utilized to detect DA in injections with a recovery of 98.50–101.25 %.

Table 4. Detection of DA in injection samples (n = 3) at $MnCr_2O_4$ nanocomposites/MCPE

Sample	Content (mg/mL)	Found (mg/mL)	RSD (%)	Recovery (%)
1	4.0	3.94	2.2	98.50
2	4.0	3.97	3.9	99.25
3	4.0	4.05	2.5	101.25

4. Conclusions

$MnCr_2O_4$ nanocomposites were synthesized by hydrothermal method, in which $MnCr_2O_4$ nanocomposites/MCPE with an average size 100nm was characterized by XRD, EDX, IR and

Annals of R.S.C.B., ISSN: 1583-6258, Vol. 25, Issue 4, 2021, Pages. 17361-17376
Received 20 May 2021; Accepted 03 June 2021

SEM analysis. $MnCr_2O_4$ nanocomposites/MCPE was prepared and several kinetic parameters were evaluated. The modified electrode exhibits increase in heterogeneous rate constant (k^0) with increase in scan rate. The electrode process was controlled by diffusion. The low detection limit was found to be 0.63 μM and compared with previous literatures found. Wide linear range (10 μM to 90 μM), the pH studies revealed that equal number of electrons and protons involved in the reaction. The proposed methods has efficiently used for the detection of DA in injections with recovery in the range 98.50–101.25%. Hence, $MnCr_2O_4$ nanocomposites/MCPE was acting as an electrochemical sensor. This work offered a simple and easy approach towards sensitive detection of DA and this method was extending to other neurotransmitters.

Acknowledgement

The author Priyanka S. R is gratefully acknowledges the financial support from Ministry of Tribal Affairs, New Delhi, INDIA under National Fellowship and Scholarship for Higher Education of ST Students to pursue Ph.D. Degree. Award Letter No. 201718-NFST-KAR-02320.

References

[1] Wightman, R.M., May, L.J., & Michael, A.C. (1998). Detection of dopamine dynamics in the brain. *Analytical Chemistry*, 60(13), 769A–779A.

[2] Mo, J.W., & Ogorevc, B. (2001). Simultaneous measurement of dopamine and ascorbate at their physiological levels using voltammetric microprobe based on overoxidized poly (1,2-phenylenediamine)-coated carbon fiber. *Analytical Chemistry*, 73(6), 1196–1202.

[3] Kim , B., Song, H. S., Jin,H. J., Park, E. J., Lee, S. H., Lee, B. Y., Park, T. H., & Hong. S., (2013). Highly selective and sensitive detection of neurotransmitters using receptor-modified single-walled carbon nanotube sensors. *Nanotechnology*, 24(28), 285501.

[4] Palanisamy. S., (2014). Simultaneous electrochemical detection of dopamine and uric acid over ceria supported three dimensional gold nanoclusters. *Materials Research Express*, 1, 045020.

[5] Howell, L. L., & Cunningham, K. A., (2015). Serotonin 5-HT_2 receptor interactions with dopamine function: Implications for therapeutics in cocaine use disorder. *Pharmacological Reviews*, 67(1), 176-197.

[6] Kaya, C., Block, E. R., Sorkin, A., Faeder, J. R. & Bahar, I. (2015). Multi-Scale Spatial Simulations Reveal the Effect of Dopamine Transporter Localization on Dopamine Neurotransmission. *BpJ*,110(3), 632a.

[7] Meyyappan, M., (2015). Nano biosensors for neurochemical monitoring. *Nano Convergence*, 2, 18.

[8] Sangamithirai, D., Munusamy, S., Narayanan, V. & Stephen, A. (2016). Fabrication of neurotransmitter dopamine electrochemical sensor based on poly(o-anisidine)/CNTs nanocomposite. *Surfaces and Interfaces*, 4, 27–34.

[9] Dhanasekaran, T., Padmanaban, A., Gnanamoorthy, G., Manigandan, R., Praveen Kumar, S., Stephen, A., & Narayanan, V. (2018). Recent advances in polymer supporting layered double hydroxides nanocomposite for electrochemical biosensors. *Materials Research Express*,5(1), 014011.

[10] Buddhala, C., Loftin, S. K., Kuley, B. M., Cairns, N. J., Campbell, M. C., Perlmutter, J. S., & Kotzbauer P.T.(2015). Dopaminergic, serotonergic, and noradrenergic deficits in Parkinson disease. *Annals of Clinical and Translational Neurology*, 2(10) 949–959.

[11] Howes, O. D., McCutcheon, R., Owen, M. J. & Murray, R. M. (2017). The Role of Genes, Stress, and Dopamine in the Development of Schizophrenia. *Biological Psychiatry*, 81, 9–20.
[12] Schulz-Schaeffer, W. (2015). Is Cell Death Primary or Secondary in the Pathophysiology of Idiopathic Parkinson's Disease? *Biomolecules.*5, 1467–1479.
[13] Petzinger, G.M., Holschneider, D.P., Fisher, B.E., McEwen, S., Kintz, N., Halliday, M., Toy, W., Walsh, J.W., Beeler, J., & Jakowec M.W. (2015). The Effects of Exercise on Dopamine Neurotransmission in Parkinson's disease: Targeting Neuroplasticity to Modulate Basal Ganglia Circuitry. *Brain Plasticity,*1(1), 29–39.
[14] Sitte, H. H., Pifl, C., Rajput, A. H., Hörtnagl, H., Tong , J., Lloyd, G. K., Kish ,S. J., Hornykiewicz , O. (2017). Dopamine and noradrenaline, but not serotonin, in the human claustrum are greatly reduced in patients with Parkinson's disease: possible functional implications. *European Journal of Neuroscience,* 45(1), 192–197.
[15] Choi, W.S., Kim, H.W., Tronche, F., Palmiter, R. D., Storm, D. R., & Xia, Z. (2017). Conditional deletion of Ndufs4 in dopaminergic neurons promotes Parkinson's disease-like non-motor symptoms without loss of dopamine neurons. *Scientific Reports*, 7, 44989.
[16] Yi, X., Wu, Y., Tan, G., Yu, P., Zhou, L., Zhou, Z., Chen, J., Wang, Z., Pang J., & Ning, C. (2017). Palladium nanoparticles entrapped in a self-supporting nanoporous gold wire as sensitive dopamine biosensor. *Scientific Reports*, 7(1), 7941.
[17] Li, J., & Lu, J. (1997). Flow-injection/chemiluminescene assays of catecholamines. *Chinese Journal of Analytical Chemistry,* 25, 314-316.
[18] Nohta, H., Yukizawa, T., Ohkura, Y., Yoshimura, M., Ishida, J., & Yamaguchi, M. (1997). Aromatic glycinonitriles and methylamines as pre-column fluorescene derivatization reagents for catecholamines. *Analytica Chimica Acta,* 344, 233-240.
[19] Wu, Y., Fan, R., & Di, J. (1996). Electrochemical study of electron transfer between dopamine and ferrocene at liquid/liquid interface. *Chinese Journal of Analytical Chemistry,* 24, 873-875.
[20] Zhu, R., & Kok, W. T. (1997). Determination of catecholamines and related compounds by capillary electrophoresis with postcolumn terbium complexation and sensitized luminescence detection. .*Analytical Chemistry,* 69, 4010-4016.
[21] Xiao, L. F., Chen, J., & Cha, C. S. (2000). Elimination of the interference of ascorbic acid in the amperometric detection of biomolecules in body fluid samples and the simple detection of uric acid in human serum and urine by using the powder microelectrode technique. *Journal of Electroanalytical Chemistry*, 495, 27-35.
[22] Hu, C.G., & Hu, S.S. (2004). Electrochemical characterization of cetyltrimethyl ammonium bromide modified carbon paste electrode and the application in the immobilization of DNA, *Electrochimica Acta,* 49(3), 405-412.
[23] Song, N. N., Wang, Y. Z., Yang, X.Y., Zong, H. L., Chen, Y. X., Ma, Z., & Chen, C.X. (2020). A novel electrochemical biosensor for the determination of dopamine and ascorbic acid based on graphene oxide/poly(aniline-co-thionine) nanocomposite, *Journal of Electroanalytical Chemistry,* 873, 114352.
[24] Viswanath, C.C., & Kumara Swamy, B.E. (2016). Sodium Alpha Olefin Sulfonate Modified Carbon Paste Electrode Sensor for Dopamine: A Voltammetric Study, *Insights in Analytical Electrochemistry,* 2, 1.

[25] Tanuja, S.B., Kumara Swamy, B.E., & Vasantakumar Pai, K. (2016).Cyclosporine/ SDS Modified Carbon Paste Electrode for Electrochemical Study of Dopamine: A Cyclic Voltammetric Study. *Insights Anal Electrochem*, 2, 2.

[26] Mahanthesha, K.R., Swamy, B.E.K., Chandra, U., Shankar S. S., & Pai, K.V. (2012). Electrocatalytic Oxidation of Dopamine at Murexide and TX-100 Modified Carbon Paste Electrode: A Cyclic Voltammetric Study, *Journal of Molecular Liquids* 172 119-124.

[27] Reddy, S., Swamy, B. E. K., & Jayadevappa, H. (2012). CuO nanoparticle sensor for the electrochemical determination of dopamine, *Electrochimica Acta*, 61, 78-86.

[28] Maleh, H. K., Ahanjan, K., Taghavi, M., & Ghaemy, M. (2016). A novel voltammetric sensor employing zinc oxide nanoparticles and a new ferrocene-derivative modified carbon paste electrode for determination of captopril in drug samples, *Analytical Methods* 8, 1780–1788.

[29] Santhosh Bullapura Matt., Shivakumar. Manjunatha., S. Manjunatha., Dharmaprakash M. Sidlingappa., and Manjappa. Sidlingappa., (2019). Synthesis of Cerium-Doped Zirconia Nanoparticles for the Electrochemical Detection of Dopamine by Modified Carbon Paste Electrode, *ChemistrySelect 4*, 5839 –5844

[30] Santhosh Bullapura Matt., Manjunatha. Shivanna., Shivakumar. Manjunatha., Manjappa. Sidlingappa Dharmaprakash Mallenahalli. Sidlingappa., and., (2020). Electrochemical Detection of Serotonin Using t-ZrO_2 Nanoparticles Modified Carbon Paste Electrode, Journal of The Electrochemical Society, 167, 155512.

[31] Vafafard, A., Goharshenasan, S., Nozari, N., Mortezapour, A., & Mahmoudi, M. (2013). Phase-dependent optical bistability in the quantum dot nanostructure molecules via inter-dot tunneling, *Journal of Luminescence*, 134, 900-905.

[32] Rangasamy, M. (2011) Nano technology: a review, *Journal of Applied Pharmaceutical Science*, 1(2), 8-16.

[33] Cole, S. W., Korin, Y. D., Fahey, J. L., & Zack, J. A. (1998). Norepinephrine Accelerates HIV Replication Via Protein Kinase A-Dependent Effects on Cytokine Production, *The Journal of Immunology*, 161(2), 610-616.

[34] Rahman, G., Mian, S.A., Shah, A.A., & Joo, O. (2016). Electrocatalytic behavior of glassy carbon electrode modified with ruthenium nanoparticles and ruthenium film, *Journal of Applied Electrochemistry*, 46, 459–468.

[35] Tong, Y., Ma, J., Zhao, S., Huo, H., & Zhang, H. (2015). A Salt-Assisted Combustion Method to Prepare Well-Dispersed Octahedral $MnCr_2O_4$ Spinel Nanocrystals, *Journal of Nanomaterials*, 214978.

[36] Afzal, A., Atiq, S., Saleem, M., Ramay. S. M., Naseem, S., & Siddiqi, S. A. (2016). Structural and magnetic phase transition of sol–gel-synthesized Cr_2O_3 and $MnCr_2O_4$ nanoparticles, *Journal of Sol-Gel Science and Technology*, DOI 10.1007/s10971-016-4066-4

[37] Song, F. L., Huang, L. R., Chen, D. H., & Tang, W. (2008) "Preparation and characterization of nanosized Zn-Co spinel oxide by solid state reaction method," *Materials Letters*, 62(3), 543–547.

[38] Santhosh B. M., Manjunatha S., Shivakumar M., Dharmaprakash M. S., and Manjappa S. (2020). Electrochemical Investigation of Caffeine by Cerium Oxide Nanoparticle Modified Carbon Paste Electrode, Journal of The Electrochemical Society, 167, 047503.

[39] Mahanthesha, K. R., Swamy, B. E. K., & Priyanka, S. R. (2018). Pretreated/Graphite pencil electrode based Electrochemical sensors for the detection of Adenosine in presence of Adenine, *International Journal of Research and Analytical Reviews*, 5, 1691-1702.

[40] Mahanthesha, K. R., Swamy, B. E. K., & Priyanka, S. R. (2018). Voltammetric resolution of Adenosine at Pretreated/Graphite pencil electrode: A Cyclic Voltammetric Study, *Journal of Emerging Technologies and Innovative Research*, 5, 15-23.

[41] Mahanthesha, K. R., Swamy, B. E. K., & Chandra, U. (2018). Simultaneous determination of dopamine at poly (Pyrogallol) modified carbon paste electrode: A Voltammetric Study, *International Journal of Research and Analytical Reviews*, 5, 1252-1257.

[42] Santhosh Bullapura Matt., S. Raghavendra., Manjunatha Shivanna., Manjappa Sidlinganahalli., Dharmaprakash Mallenahalli Siddalingappa.,(2020). Electrochemical Detection of Paracetamol by Voltammetry Techniques Using Pure Zirconium Oxide Nanoparticle Based Modified Carbon Paste Electrode, Journal of Inorganic and Organometallic Polymers and Materials, 31, 511-519.

[43] Mahanthesha, K. R., Swamy, B. E. K., Chandra, U., Reddy, S., & Pai, K. V. (2014). Sodium dodecyl sulphate/polyglycine/phthalamide/carbon paste electrode based voltammetric sensors for detection of dopamine in the presence of ascorbic acid and uric acid, *Chemical Sensors*, 4, 1–7.

[44] Raoof, J. B., Kiani, A., Ojani, R., & Valiollahi, R. (2011). Electrochemical Determination of Dopamine Using Banana-MWCNTs Modified Carbon Paste Electrode, *Analytical and Bioanalytical electrochemistry.*, 3(1), 59-66.

[45] Zhu, Z., Qu, L., Guo, Y., Zeng, Y., Sun, W., & Huang, X. (2010). Electrochemical detection of dopamine on a Ni/Al layered double hydroxide modified carbon ionic liquid electrode, *Sensors and Actuators B: Chemical*, 151(1), 146-152.

[46] Avendano, S. C., Silva, M. T. R., Pardave M. P., Martinez L. H., Romo, M. R., & Angles, G. A. (2010). Influence of CTAB on the electrochemical behavior of dopamine and on its analytic determination in the presence of ascorbic acid, *Journal of Applied Electrochemistry.*, 40, 463-474.

[47] Wang, Q., Li, N., & Wang, W., (2002). Electrocatalytic response of dopamine at a metallothioneins self-assembled gold electrode. *Analytical sciences: the international journal of the Japan Society for Analytical Chemistry*, 18(6), 635-9.